

Simulations of Shikimate Dehydrogenase from
Mycobacterium tuberculosis in Complex with 3-
dehydroshikimate and NADPH Suggest Strategies for
*Mtb*SDH inhibition

Auradee Punkvang^{a,}, Pharit Kamsri^a, Adrian Mulholland^b, James Spencer^c, Supa
Hannongbua^d, and Pornpan Pungpo^e*

^aFaculty of Science, Nakhon Phanom University, 48000 Nakhon Phanom, Thailand

^bSchool of Chemistry, University of Bristol, Clifton, BS8 1TS Bristol, United Kingdom

^cSchool of Cellular and Molecular Medicine, University of Bristol, Bristol BS8 1TD, United Kingdom

^dDepartment of Chemistry, Faculty of Science, Kasetsart University, Chatuchak, 10900 Bangkok, Thailand

^eDepartment of Chemistry, Faculty of Science, Ubon Ratchathani University, Warinchamrap, 34190 Ubon Ratchathani, Thailand

*E-mail: auradee.punkvang@npu.ac.th

Table S1. The total number of atoms in all systems for MD simulation.

MD system	Total atoms of system
apo <i>Mtb</i> SDH	31,770
DHS/ <i>Mtb</i> SDH	31,798
DHS/NADPH/ <i>Mtb</i> SDH	31,743
DHS/K69A <i>Mtb</i> SDH	31,726
DHS/D105N <i>Mtb</i> SDH	31,803
DHS/NADPH/K69A <i>Mtb</i> SDH	31,722
DHS/NADPH/D105N <i>Mtb</i> SDH	31,748
DHS/ <i>proR</i> -NADPH/ <i>Mtb</i> SDH	31,764
DHS/ <i>proR</i> NADPH /A213L <i>Mtb</i> SDH	31,773

Table S2. Cluster number and the percent occurrence of the most populated cluster obtained from three MD simulations of *Mtb*SDH systems

System	1 st MD simulation		2 nd MD simulation		3 rd MD simulation	
	Cluster number	%occurrence ^a	Cluster number	%occurrence	Cluster number	%occurrence
apo <i>Mtb</i> SDH	7	44^b	10	33	16	19
DHS/ <i>Mtb</i> SDH	4	49^b	4	42	10	23
DHS/K69A <i>Mtb</i> SDH	13	18	11	22	7	39^b
DHS/D105N <i>Mtb</i> SDH	8	48^b	10	25	12	27
DHS/NADPH/ <i>Mtb</i> SDH	5	37	2	60	2	78^b
DHS/NADPH/K69A <i>Mtb</i> SDH	9	24^b	16	19	12	16
DHS/NADPH/D105N <i>Mtb</i> SDH	7	28	6	29^b	12	19
DHS/ <i>proR</i> -NADPH / <i>Mtb</i> SDH	4	51^b	9	25	14	21
DHS/ <i>proR</i> NADPH /A213L <i>Mtb</i> SDH	4	35	2	95^b	4	47

^aThe percent occurrence of the most populated cluster, the representative snapshot in this cluster was selected as the representative structure of each MD simulation.

^bThe highest percent occurrence of the most populated cluster among three MD simulations of each system. The representative structure in this cluster was used as the representative structure of each *Mtb*SDH systems.

Table S3. RMSD values of three backbone structures of *Mtb*SDH obtained from three MD simulations of each system

MD system	RMSD (Å) ^a		
	1 st and 2 nd simulations	1 st and 3 rd simulations	Average
apo <i>Mtb</i> SDH	1.11	1.03	1.07
DHS/ <i>Mtb</i> SDH	1.31	1.14	1.23
DHS/NADPH/ <i>Mtb</i> SDH	1.15	1.13	1.14
DHS/K69A <i>Mtb</i> SDH	1.21	1.03	1.12
DHS/D105N <i>Mtb</i> SDH	1.34	1.31	1.33
DHS/NADPH/K69A <i>Mtb</i> SDH	1.49	1.26	1.38
DHS/NADPH/D105N <i>Mtb</i> SDH	1.09	1.78	1.44
DHS/ <i>proR</i> -NADPH/ <i>Mtb</i> SDH	1.04	1.11	1.08
DHS/ <i>proR</i> NADPH /A213L <i>Mtb</i> SDH	1.04	1.33	1.19

^aThree representative structures obtained from three MD simulations of each system were superimposed by Swiss-PdbViewer 4.1.0. Then, RMSD values of between all backbone atoms of *Mtb*SDH obtained from first and second simulations (1st and 2nd simulation) and from first and third simulations (1st and 3rd simulation) were calculated and averaged.

1. Stability of MD simulation systems

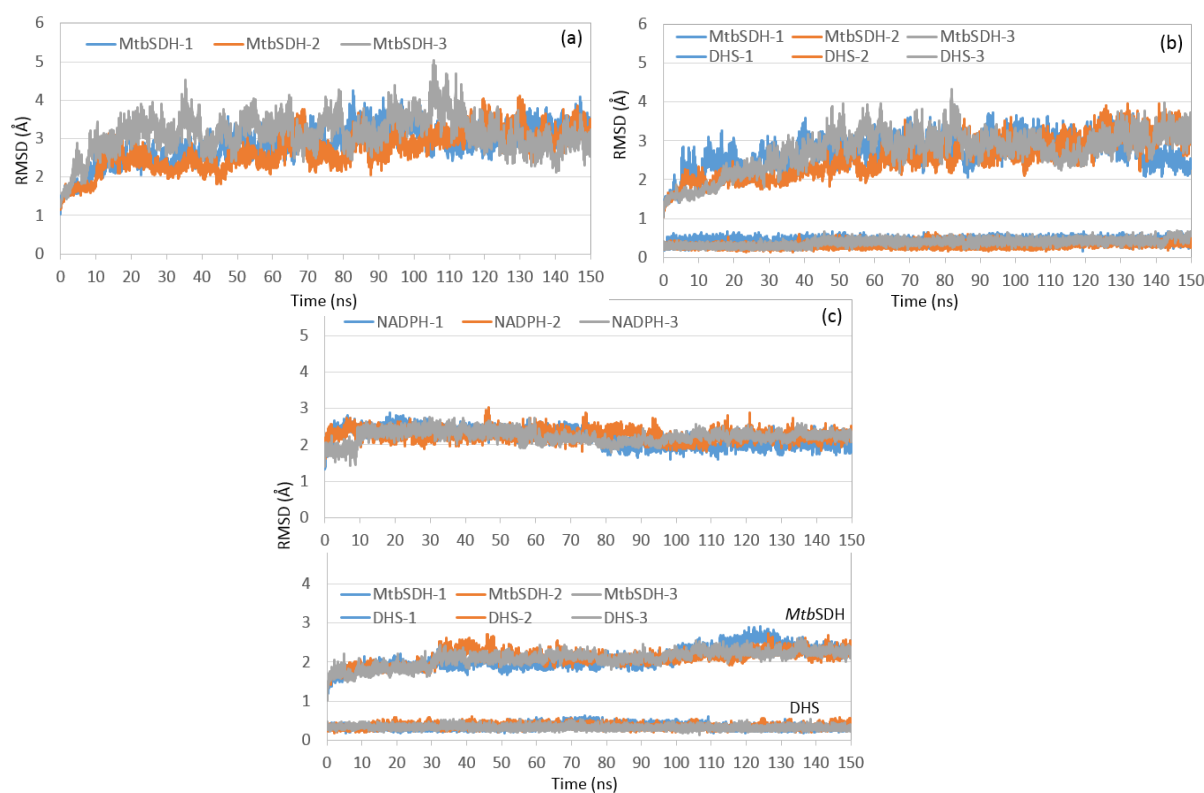


Figure S1. The RMSD plots of all atoms of DHS, NADPH and *Mtb*SDH in three MD simulations of apo *Mtb*SDH (a), binary DHS/*Mtb*SDH (b) and ternary DHS/NADPH/*Mtb*SDH (c) over 150 ns simulation time.

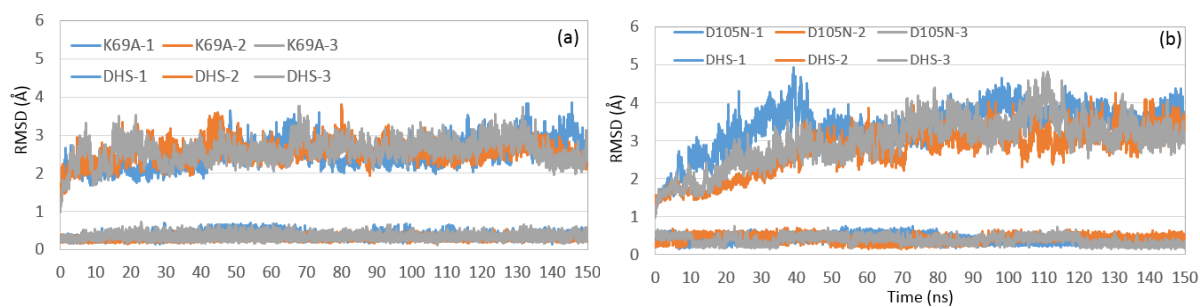


Figure S2. The RMSD plots of all atoms of DHS and mutant *MtbSDH* in three MD simulations of DHS/K69A *MtbSDH* (a), DHS/D105N *MtbSDH* (b) over 150 ns simulation time.

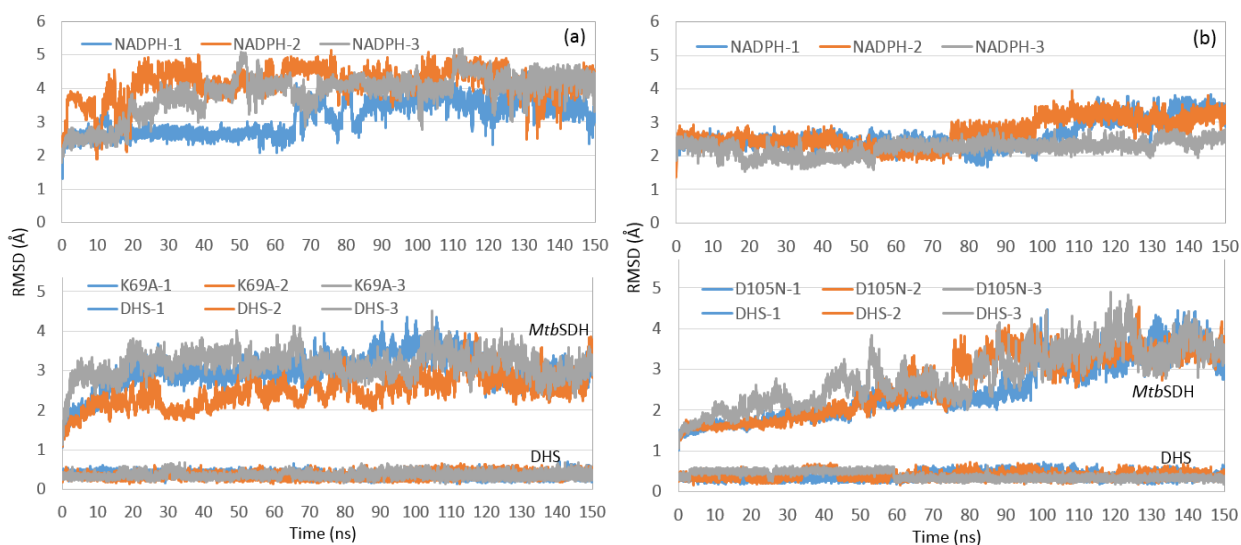


Figure S3. The RMSD plots of all atoms of DHS, NADPH and mutant *MtbSDH* in three MD simulations of DHS/NADPH/K69A *MtbSDH* (a) and DHS/NADPH/D105N *MtbSDH* (b) over 150 ns simulation time.

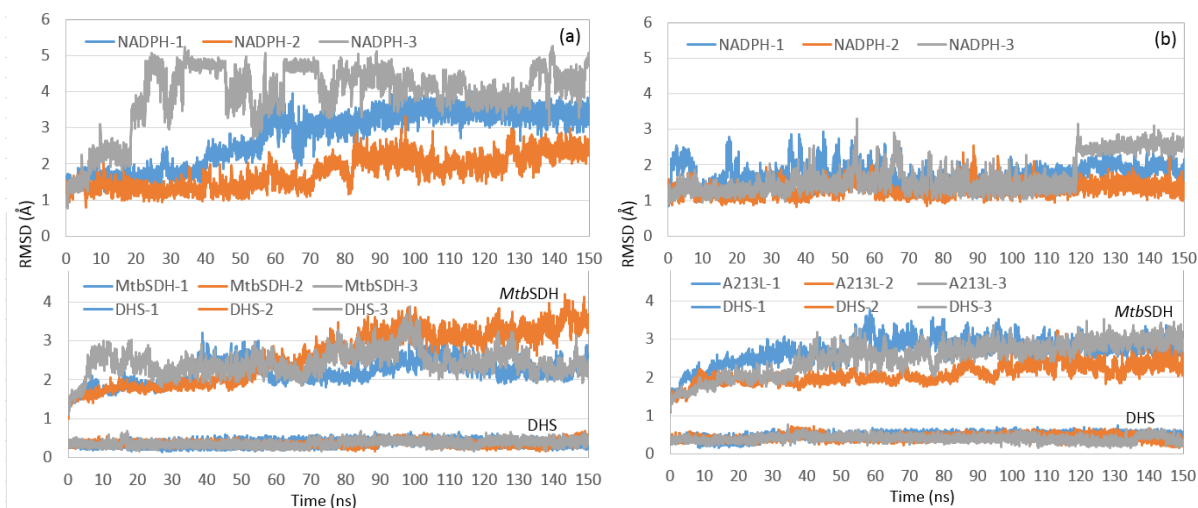


Figure S4. The RMSD plots of all atoms of DHS, NADPH and *MtbSDH* in three MD simulations of DHS/*proR*-NADPH/*MtbSDH* (a) and DHS/*proR* NADPH/A213L *MtbSDH* (b) over 150 ns simulation time.

2. Flexibility of *Mtb*SDH

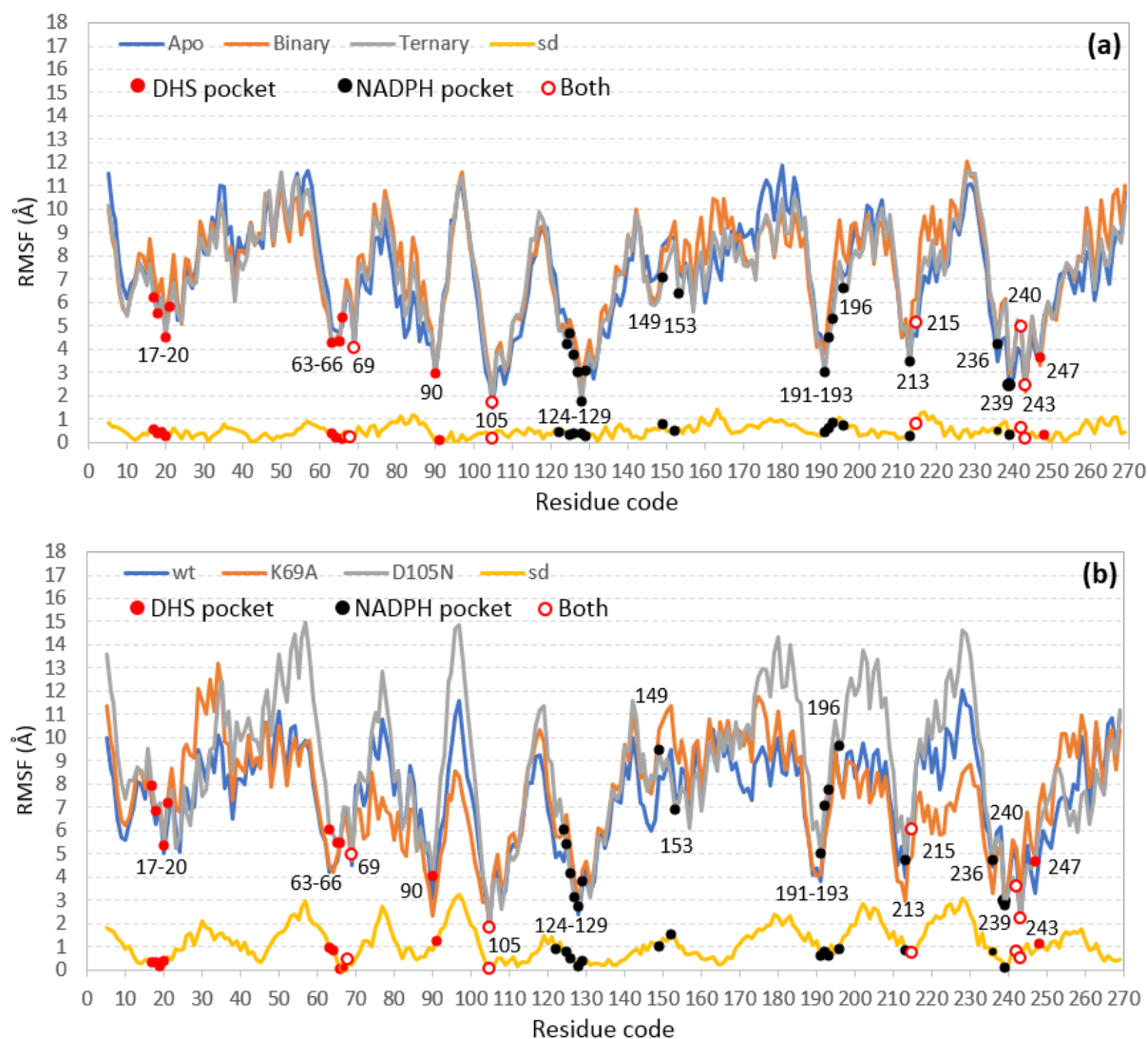


Figure S5. Global Flexibility of *Mtb*SDH and Complexes. RMSF visualizations of (a), ligand-unbound *Mtb*SDH (apo *Mtb*SDH) and ligand-bound *Mtb*SDH (binary DHS/*Mtb*SDH and ternary DHS/NADPH/*Mtb*SDH); (b), binary complexes of wild-type (DHS/*Mtb*SDH) and mutant (DHS/K69A *Mtb*SDH and DHS/D105N *Mtb*SDH) *Mtb*SDH. RMSF values were calculated for all atoms of each residue in *Mtb*SDH over the last 50 ns of MD simulations. Standard deviations (sd) of RMSF values for each *Mtb*SDH residue in the different systems were calculated to show flexibility deviations.

3. DHS binding in the binary DHS/*Mtb*SDH complex

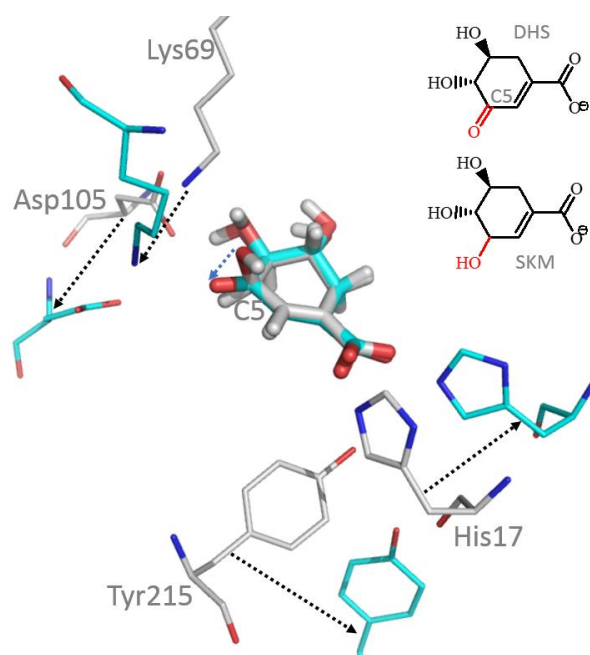


Figure S6. Rearrangement of *Mtb*SDH on DHS and SKM binding. It is obtained by the fitting only atoms of DHS in DHS/*Mtb*SDH complex structure modeled here by MD simulation on those SKM in SKM/*Mtb*SDH (PDB code 4P4G). Carbon atoms of DHS/*Mtb*SDH structure are cyan colored and those of SKM/*Mtb*SDH are gray. Black dotted arrows indicate direction of movement of residues.

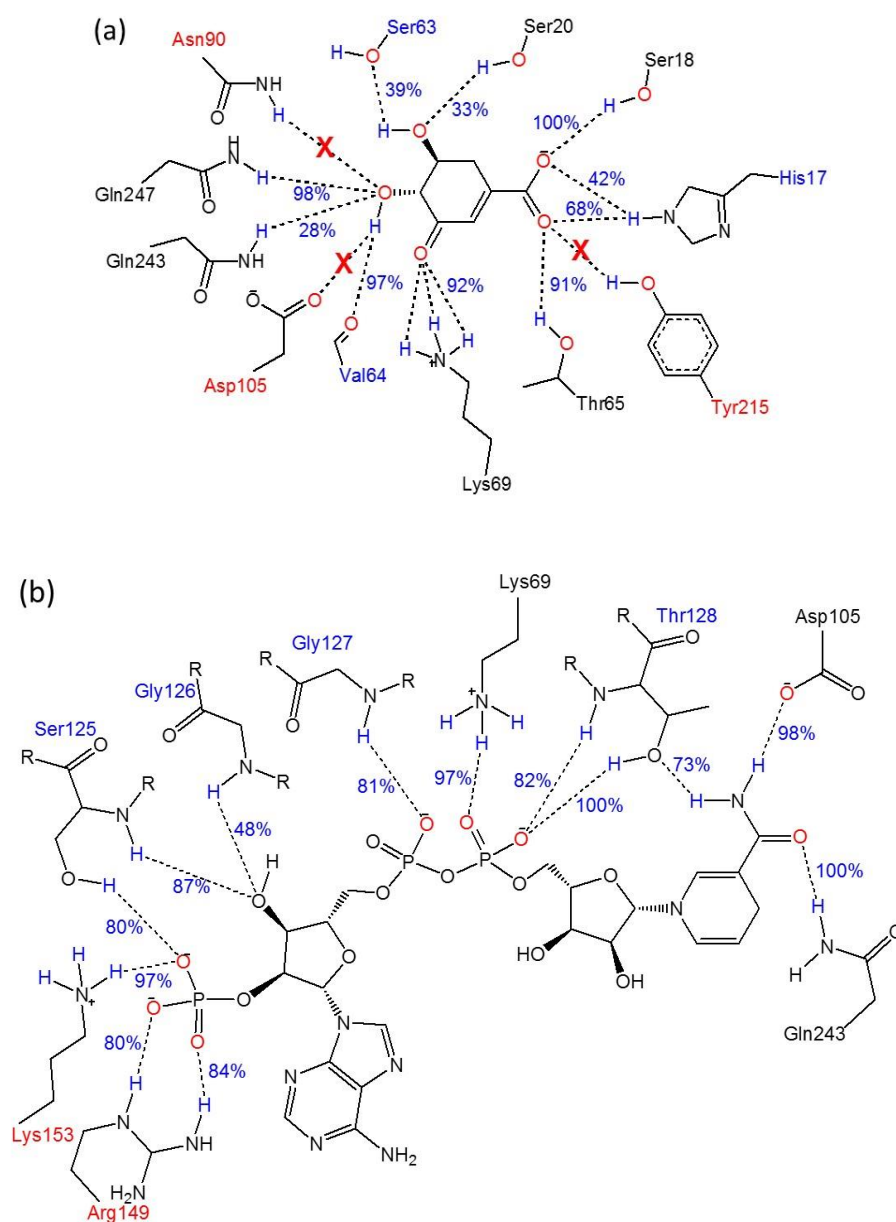


Figure S7. Hydrogen bond analysis of DHS and NADPH binding in *MtbSDH* complexes. (a) model derived here from MD simulation compared to SKM binding in SKM/*MtbSDH* crystal structure (PDB code 4P4G). Percentage figures indicate % occupation of each hydrogen bond for DHS binding over the equilibrium state of MD simulation. Residues labeled in black make hydrogen bonds to both SKM and DHS. Residues labeled in red make hydrogen bonds to SKM, and residues labeled blue to DHS, only. (b) Hydrogen bonding pattern and % occupation for NADPH binding in the representative structure of DHS/NADPH/*MtbSDH* ternary complex modeled from MD simulations. Residues labeled in red form the electrostatic clamp and in blue the diphosphate-binding loop.

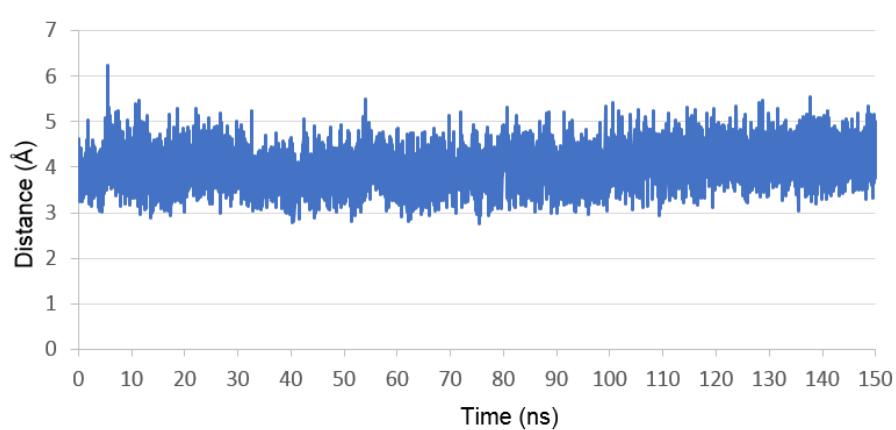


Figure S8. The distance between the *proS* hydrogen atom of NADPH and the DHS carbonyl carbon monitored over the 150ns simulation time

4. Selection of *proS* conformation of NADPH nicotinamide ring

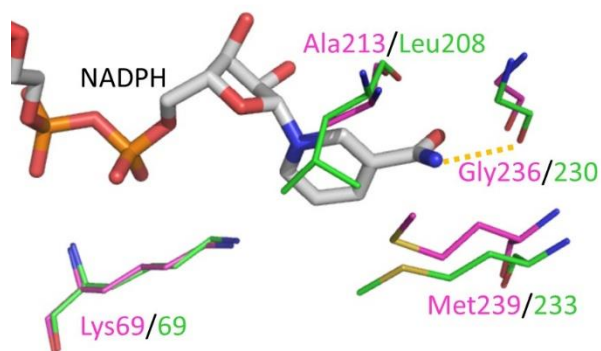


Figure S9. Binding sites for the NADPH nicotinamide ring in *M. tuberculosis* and *H. pylori* SDH. Figure shows *MtbSDH* (PDB 4P4G, carbon atoms pink) and *H. pylori* SDH (PDB 3PHI, carbon atoms green) with NADPH from *H. pylori* SDH. (carbon atoms gray).

5. Roles of Lys69 and Asp105 in DHS and NADPH binding by *Mtb*SDH

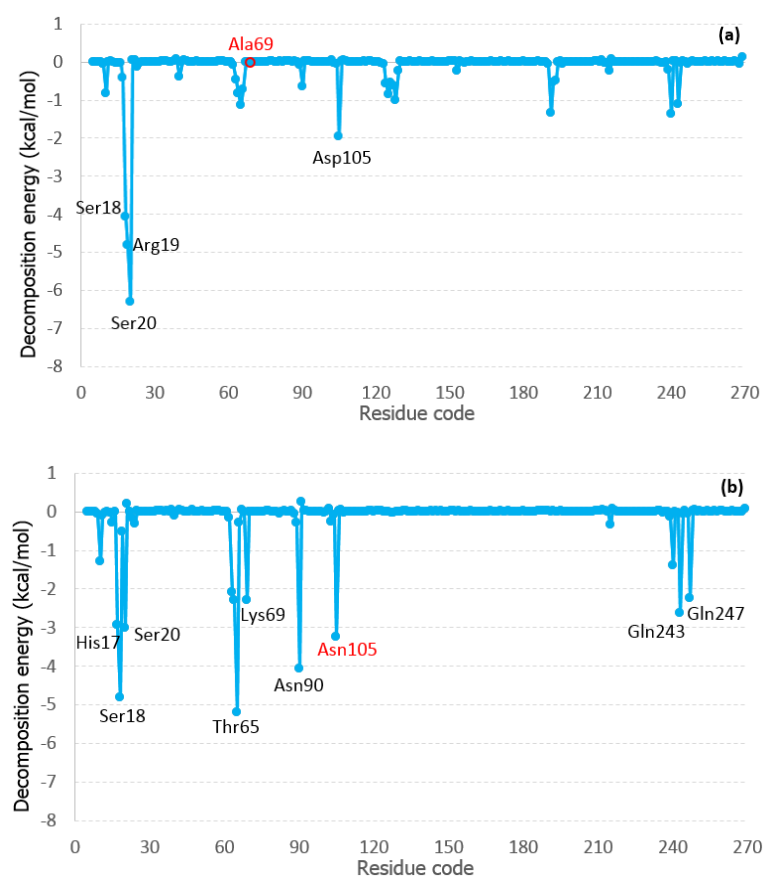


Figure S10. The influence of K69A and D105N mutations on the decomposition energy of DHS in binary DHS/*Mtb*SDH complex. (a) and (b), Plots of MM-GBSA decomposition energy showing contribution of each *Mtb*SDH residue to DHS binding in DHS/K69A *Mtb*SDH and DHS/D105N complexes, respectively.